DOI: ADD DOINUMBER HERE

On the minimum time optimal control problem of an aircraft in its climbing phase

O. Cots[⋆], *P. Delpy*[‡], *J. Gergaud*[⋆] *and D. Goubinat*[⋆†]
[⋆] *Toulouse Univ., INP-ENSEEIHT, IRIT & CNRS, 2 rue Camichel, F-31071 Toulouse, France*
[‡] *Thales Avionics SA, 105 av du General Eisenhower, B.P. 1147, 31047 Toulouse Cedex, France*
[†]damien.goubinat@enseeiht.fr

Abstract

In this article, the minimum time optimal control problem of an aircraft in its climbing phase is studied. First, a reduction of the initial dynamics into a three dimensional single-input system with a linear dependence with respect to the control is performed. This reduced system is then studied using geometric control techniques. In particular, the maximum principle leads to describe a multi-point boundary value problem which is solved by indirect methods. These methods are the implementation of the maximum principle and are initialized by direct methods. We check that the extremal solution of the boundary value problem satisfies necessary and sufficient conditions of optimality. From this reference case and considering small-time optimal trajectories, we give a local classification with respect to the initial mass and final velocity of BC-extremals for the climbing phase.

1. Introduction

An aircraft travels along several phases during a flight. These phases are the take-off, the climb, the cruise, the descent, the approach and the landing. In this article, we are interested in the time-optimal control problem of an aircraft in its climbing phase. This phase is determined by its own dynamics and governed by a system of ordinary differential equations of dimension 4. The aircraft is represented by the altitude h, the true air speed v, the mass m and the air slope γ. The performance model which describes the evolution of the thrust, the fuel flow and the drag coefficient is a Base of Aircraft Data (BADA) model from Eurocontrol.[19] The atmospheric data as the pressure, the temperature and the air density are given by the International Standard Atmosphere (ISA) model. In our model, the lift coefficient is taken as the control variable.

The climbing phase has already been studied by the NASA.[2,18] These works higlight a time scale separation between the different state variables. In his work, Ardema[2] classified the air slope γ as a very fast variable, the true air speed v and the altitude h as fast variables and the mass m as a slow variable. This time scale separation between the variables is tackled by a singular perturbation analysis. The method used here to deal with the singular perturbation consists in turning the system of ordinary differential equations into a system of differential algebraic equations by taking a quasi-steady approximation of the very fast variable γ. Numerically, this technique gives a very good approximation of the original time-to climb problem[10] and leads to the reduction of the dynamics into a single-input dynamics of dimension 3 with a linear dependence with respect to the control. In this reduced problem, the new control variable is the air slope γ. This reduced problem is then studied through the Pontryagin's Maximum Principle[20] (PMP) and second-order optimality conditions. The extremals solution of the maximum principle are classified using the work of Bonnard and Kupka.[7] From this work and thanks to small-time analysis a local classification of time-optimal trajectories is sketched.

The paper is organized as follows. The physical model with the optimal control problem are defined in section 2. In section 3, we analyze the optimal control problem with the application of the maximum principle and we classify the bang-bang extremals near the switching surface in the particular case of the dimension 3. Then, in section 4, a local time-optimal classification is sketched thanks to numerical methods and small-time considerations.

2. Physical model and Mayer optimal control problem

In this section, we present the dynamics of the climbing phase. We restrict the dynamics to the vertical motion of the aircraft. The aircraft is subjected to four forces, the drag $\overrightarrow{D}$, the lift $\overrightarrow{L}$, the thrust $\overrightarrow{T}$ and its own weight $\overrightarrow{P}$. We use a

nonlinear point mass representation and we consider that all the forces apply on the center of gravity of the aircraft. Let assume that the thrust, the drag and the velocity vector $\vec{V}$ are colinear. The application of the first dynamics principle, assuming that the earth system is galilean, provides the following four dimensional system:

$$\dot{h} = v\sin(\gamma), \tag{1}$$

$$\dot{v} = \frac{T}{m} - \frac{1}{2}\frac{\rho S v^2}{m}C_D - g_0\sin(\gamma), \tag{2}$$

$$\dot{m} = -C_s T, \tag{3}$$

$$\dot{\gamma} = \frac{1}{2}\frac{\rho S v}{m}C_L - \frac{g}{v}\cos(\gamma), \tag{4}$$

where the state variables h, v, m and γ represent respectively the altitude, the velocity, the mass and the air slope. In this model, the fuel flow C_s, the thrust T and the drag coefficient C_D are given by the BAse of Aircraft Data[19] model:

$$C_s(v) \coloneqq C_{s,1}\left(1 + \frac{v}{C_{s,2}}\right), \quad T(h) \coloneqq C_{t,1}\left(1 - \frac{h}{C_{t,2}} + h^2 C_{t,3}\right), \quad C_D \coloneqq C_{D,0} + C_{D,1}C_L^2,$$

where the constants $C_{s,i}$, $C_{t,i}$ and $C_{D,i}$ are specific to the aircraft. The International Standard Atmospheric model provides the expression of the pressure P, the temperature Θ and the air density ρ:

$$P(h) \coloneqq P_0\left(\frac{\Theta(h)}{\Theta_0}\right)^{g_0/(\beta R)}, \quad \Theta(h) \coloneqq \Theta_0 - \beta h, \quad \rho(h) \coloneqq \frac{P(h)}{R\Theta(h)}.$$

The remaining data are positive constants: g_0 is the gravitational constant, S the wing area, R the specific constant of air, β the thermical gradient and P_0, Θ_0 represent the pressure and temperature at the sea level.

Regarding the lift coefficient C_L as the control variable looks like a natural idea in the considered dynamics. However, according to the work of Ardema[2] and Nguyen,[18] the dynamics contains slow (the mass m), fast (the altitude h and the velocity v) and very fast variables (the air slope γ). The time scale separation between the slow and the very fast variable is handled by a singular perturbation analysis which consists here in taking the very fast variable as the new control variable and replacing its corresponding dynamics by a quasi-steady approximation:

$$0 = \frac{1}{2}\frac{\rho S v}{m}C_L - \frac{g}{v},$$

where we also consider that the air slope remains small (from 0 to $\gamma_{\max} \coloneqq 0.262$ radians) so we set $\cos(\gamma) \approx 1$ and $\sin(\gamma) \approx \gamma$. These assumptions lead to the following affine controlled dynamics:

$$\dot{x}(t) = f_0(x(t)) + u(t)\, f_1(x(t)),$$

where $x \coloneqq (h, v, m)$, $u \coloneqq \gamma$,

$$f_0(x) \coloneqq \begin{pmatrix} 0 \\ \dfrac{T(h)}{m} - \dfrac{1}{2}\dfrac{\rho S v^2}{m}C_{D,0} + \dfrac{2mg_0}{\rho S v^2}C_{D,1} \\ -C_s T(h) \end{pmatrix} \quad \text{and} \quad f_1(x) \coloneqq \begin{pmatrix} v \\ -g_0 \\ 0 \end{pmatrix}.$$

A previous work[10] has shown that this reduced system is a very good approximation of the original dynamics. Finally, the time-optimal climbing problem is defined by:

$$\left|\begin{array}{l} \min\limits_{u(\cdot),\, t_f} t_f, \\ \dot{x}(t) = f_0(x(t)) + u(t)\, f_1(x(t)), \quad |u(t)| \leqslant u_{\max}, \quad \forall t \in [0\,, t_f] \text{ a.e.}, \quad x(0) = x_0, \\ b(x(t_f)) = 0, \end{array}\right. \tag{$\mathcal{P}_{t_f}$}$$

where $u_{\max} \coloneqq \gamma_{\max}$, $x_0 \coloneqq (h_0, v_0, m_0)$ and $x_f \coloneqq (h_f, v_f, m_f)$ are totally determined and where

$$b(x) \coloneqq \begin{pmatrix} h - h_f \\ v - v_f \\ m - m_f \end{pmatrix}.$$

3. Analysis of the time-optimal problem using the maximum principle

3.1 Necessary optimality conditions and singular trajectories

Let define the pseudo-Hamiltonian of the Mayer optimal control problem $(\mathcal{P}_{t_f})$

$$\begin{aligned} H\colon \mathbb{R}^n \times (\mathbb{R}^n)^* \times \mathbb{R} &\to \mathbb{R} \\ (x, p, u) &\mapsto H(x, p, u) \coloneqq \langle p\,, f_0(x)\rangle + u\,\langle p\,, f_1(x)\rangle\,. \end{aligned}$$

If $(\bar{u}(\cdot), \bar{t}_f)$ is a solution of $(\mathcal{P}_{t_f})$ with $\bar{x}(\cdot)$ the associated trajectory, then, the maximum principle[20] asserts that there exists a real number $p^0 \leqslant 0$ and an absolutely continuous function $\bar{p}(\cdot)\colon [0\,, \bar{t}_f] \to (\mathbb{R})^*$ such that $(\bar{p}(\cdot), p^0) \neq (0, 0)$. Besides, for $t \in [0\,, \bar{t}_f]$ a.e., we have

$$\dot{\bar{x}}(t) = \frac{\partial H}{\partial p}(\bar{x}(t), \bar{p}(t), \bar{u}(t)), \quad \dot{\bar{p}}(t) = -\frac{\partial H}{\partial x}(\bar{x}(t), \bar{p}(t), \bar{u}(t)), \tag{5}$$

and the maximization condition holds:

$$H(\bar{x}(t), \bar{p}(t), \bar{u}(t)) = \max_{|w|\leqslant u_{\max}} H(\bar{x}(t), \bar{p}(t), w). \tag{6}$$

For our time-optimal problem, the following boundary conditions must be fulfilled:

$$b(\bar{x}(\bar{t}_f)) = 0, \tag{7}$$

$$H(\bar{x}(\bar{t}_f), \bar{p}(\bar{t}_f), \bar{u}(\bar{t}_f)) = -p^0. \tag{8}$$

Definition 1. We call an extremal a triplet $(x(\cdot), p(\cdot), u(\cdot))$ which satisfies equations (5) and (6) and such that $H > 0$ along it. It is called a BC-extremal if it satisfies also (7) and (8).

Remark 1. We only consider extremals in the normal case ($p^0 \neq 0$), and by homogeneity we take $p^0 = -1$. Besides, for any extremal $(x(\cdot), p(\cdot), u(\cdot))$, the adjoint vector $p(\cdot)$ never vanishes.

The singular extremals play an important role in this study. A complete study of these extremals can be found in the work of Bonnard and Chyba[5] but here, we focus our analysis on a single-input affine system in dimension 3. First, we give a propostion which characterizes the singular extremals. We use this proposition as a definition of the singular extremals.

Proposition 3.1. *The control $u(\cdot)$ with its associated trajectory $x(\cdot)$ are singular on $[0\,, T]$ if and only if there exists a non zero adjoint $p(\cdot)$ such that $(x(\cdot), p(\cdot), u(\cdot))$ is solution a.e. on $[0\,, T]$ of the following equations:*

$$\begin{aligned} \dot{x}(t) &= \frac{\partial H}{\partial p}(x(t), p(t), u(t)), \\ \dot{p}(t) &= -\frac{\partial H}{\partial x}(x(t), p(t), u(t)), \\ 0 &= \frac{\partial H}{\partial u}(x(t), p(t), u(t)). \end{aligned}$$

Definition 2. Let consider a smooth manifold M and a set of local coordinates x.

- **Lie derivative.** A smooth vector field F defined on M acts on a smooth function f of M as the Lie derivative which is defined by $f \mapsto (F \cdot f)(x) \coloneqq \mathrm{d}f(x)F(x)$ for $x \in M$.
- **Lie bracket.** The Lie bracket of two smooth vector fields F_0 and F_1 defined on M, which represents the action of the vector field F_0 over F_1, is defined by $F_1 \mapsto [F_0\,, F_1] \coloneqq F_0 \cdot F_1 - F_1 \cdot F_0$, *i.e.* $[F_0\,, F_1](x) = \mathrm{d}F_0(x)F_1(x) - \mathrm{d}F_1(x)F_0(x)$.
- **Poisson bracket.** Denoting H_0 and H_1, the Hamiltonian lifts associated to F_0 and F_1, we defined by $\{H_0\,, H_1\} \coloneqq \overrightarrow{H}_0 \cdot H_1 = H_{[F_0,F_1]}$ the Poisson bracket between H_0 and H_1, where $\overrightarrow{H} \coloneqq (\partial_p H, -\partial_x H)$. We note H_{01} the Poisson bracket between H_0 and H_1 and H_{001} the Poisson bracket between H_0 et H_{01}.

In our problem, $\partial_u H = H_1 = 0$ has to be differentiated at least twice along an extremal to compute the control and one gets:

$$H_1 = H_{01} = H_{001} + u\, H_{101} = 0.$$

A singular extremal along which $H_{101} \neq 0$ is called of minimal order and the corresponding control is given by

$$u_s(z) \coloneqq -\frac{H_{001}(z)}{H_{101}(z)},$$

where $z \coloneqq (x, p)$. Plugging such u_s into H defines a true Hamiltonian, denoted h_s, whose solutions initiating from $H_1 = H_{01} = 0$ define the singular extremals of minimal order outside $H_{101} = 0$. We also have the following additional necessary conditions of optimality deduced from the high-order maximum principle.[14] If the singular control $u_s(\cdot)$ is non saturating, *i.e.* $|u_s(\cdot)| < u_{\max}$, then the generalized Legendre-Clebsch condition must hold along the associated singular extremal:

$$\frac{\partial}{\partial u}\frac{\partial}{\partial \mathrm{t}^2}\frac{\partial H}{\partial u} = H_{101} \geqslant 0. \tag{9}$$

Introducing the determinants,

$$\begin{aligned} D_0(x) &\coloneqq \det(f_1(x), f_{01}(x), f_0(x)),\\ D_{001}(x) &\coloneqq \det(f_1(x), f_{01}(x), f_{001}(x)),\\ D_{101}(x) &\coloneqq \det(f_1(x), f_{01}(x), f_{101}(x)), \end{aligned}$$

then the singular trajectories and control are given by the following proposition.

Proposition 3.2. *The singular trajectories satisfy*

$$\dot{x}(t) = f_0(x(t)) - \frac{D_{001}(x(t))}{D_{101}(x(t))} f_1(x(t)),$$

outside $\Big\{x \in \mathbb{R}^3 \;\Big|\; D_{101}(x) = 0\Big\}$.

Proof. Along a singular extremal, $H_1(z(\cdot)) \equiv 0$, so differentiating twice this quantity with respect to the time leads to

$$\langle p\,, f_1(x)\rangle = \langle p\,, f_{01}(x)\rangle = \langle p\,, f_{001}(x) + u\, f_{101}(x)\rangle = 0$$

along the extremal. Since $p(\cdot)$ does not vanish, then we have $\det(f_1(x), f_{01}(x), f_{001}(x) + u\, f_{101}(x)) = 0$ along the singular extremal and by linearity of the determinant, we obtain the expected result. □

Remark 2. In this case, the singular control is given in feedback form and we note with the same notation:

$$u_s(x) \coloneqq -\frac{D_{001}(x)}{D_{101}(x)}. \tag{10}$$

Proposition 3.3. *Along any singular extremal such that $D_0 \neq 0$ we have*

$$H_{101} \geqslant 0 \iff D_0\, D_{101} \geqslant 0.$$

Proof. Along any singular extremal $(x(\cdot), p(\cdot), u(\cdot))$, if $D_0(x) \neq 0$ then $\mathrm{span}(\{f_1(x), f_{01}(x)\})$ is a plane of $\mathbb{R}^3$ which separates this space into two half spaces and for which p is a normal vector (since $\langle p\,, f_1(x)\rangle = \langle p\,, f_{01}(x)\rangle = 0$ along the singular extremal). Besides, since $H(x, p, u) = H_0(x, p) = \langle p\,, f_0(x)\rangle > 0$ along the singular extremal, then p and $f_0(x)$ are in the same half space. At the end, $H_{101}(x, p) = \langle p\,, f_{101}(x)\rangle \geq 0$ if and only if $f_{101}(x)$ and $f_0(x)$ are in the same half space, whence the result. □

Corollary 3.4. *The strict generalized Legendre-Clebsch condition* (9) *becomes $D_0\, D_{101} > 0$ along a singular arc.*

3.2 Generic classification of the bang-bang extremal near the switching surface.

Along a singular extremal we have $\partial_u H \equiv 0$. In our particular case of a single-input affine system this condition becomes $H_1(z(t)) = 0$. Let define the sets Σ_1 and Σ_s, such that Σ_1 represents the switching surface, *i.e.* $\Sigma_1 \coloneqq \{z \coloneqq (x,p) \in \mathbb{R}^n \times (\mathbb{R}^n)^* \mid H_1(z) = 0\}$, and where $\Sigma_s \coloneqq \{z \coloneqq (x,p) \in \mathbb{R}^n \times (\mathbb{R}^n)^* \mid H_1(z) = H_{01}(z) = 0\}$ contains all the singular extremals. We define the switching function $\Phi\colon t \mapsto \Phi(t) \coloneqq H_1(z(t))$ and we note Φ_+ (resp. Φ_-) if the control along the extremal is $u_{\max}$ (resp. $-u_{\max}$). The first and second derivatives of $\Phi_\pm$ are given by:

$$\begin{aligned}\dot{\Phi}_\pm(t) &= H_{01}(z(t)),\\ \ddot{\Phi}_\pm(t) &= H_{001}(z(t)) \pm u_{\max} H_{101}(z(t)).\end{aligned}$$

Definition 3. An extremal is said bang-bang on $[0\,, t_f]$ if it is composed of a finite number of arcs of the form σ_+ and σ_- where σ_+ (resp. σ_-) represents a bang arc for which $u(\cdot) \equiv u_{\max}$ (resp. $-u_{\max}$). In a similar way, σ_s represents a singular trajectory and we denote by $\sigma_1\sigma_2$ an arc σ_1 followed by an arc σ_2.

Near the switching surface Σ_s, the behavior of the extremals for a single-input affine system is detailled in the work of Kupka.[15] We have the following:

Ordinary point. Let consider $z_0 \coloneqq (x_0, p_0) \in \Sigma_1 \setminus \Sigma_s$ and t_0 its associated time such that $z_+(t_0) = z_-(t_0) = z_0$, where $z_+(\cdot)$ (resp. $z_-(\cdot)$) represents the extremal with $u(\cdot) \equiv u_{\max}$ (resp. $u(\cdot) \equiv -u_{\max}$). According to the maximum principle, near Σ_1, the extremal is of the form $\sigma_-\sigma_+$ if $\dot{\Phi}(t_0) > 0$ and $\sigma_+\sigma_-$ if $\dot{\Phi}(t_0) < 0$.

Fold point. Let consider now a point $z_0 \in \Sigma_s$ and assume that Σ_s is a smooth manifold of codimension two. Let denote t_0 the time associated to z_0. At t_0, the extremal has a contact of order at least two with Σ_1. If the contact is exactly of order two, *i.e.* $\ddot{\Phi}_\pm(t_0) \neq 0$, then locally z_0 is a fold point and three different behaviors can be encountered.

- Parabolic case: $\ddot{\Phi}_+(t_0)\,\ddot{\Phi}_-(t_0) > 0$. The singular extremal at the switching time is not admissible and every extremal is of the form $\sigma_+\sigma_-\sigma_+$ or $\sigma_-\sigma_+\sigma_-$ with at most two switchings.
- Hyperbolic case: $\ddot{\Phi}_+(t_0) > 0$ and $\ddot{\Phi}_-(t_0) < 0$. A connection with a singular extremal is possible and locally each extremal is of the form $\sigma_\pm\sigma_s\sigma_\pm$ (by convention each arc of the sequence can be empty).
- Elliptic case: $\ddot{\Phi}_+(t_0) < 0$ and $\ddot{\Phi}_-(t_0) > 0$. In this case, a connection with a singular extremal is not possible. The elliptic trajectories are then bang-bang with no uniform bound on the number of switchings.

Let assume $D_0(x) \neq 0$, then the family $(f_0(x), f_1(x), f_{01}(x))$ forms a basis of $\mathbb{R}^3$ and there exists $(\alpha, \alpha_1, \alpha_{01}) \in \mathbb{R}^3$ and $(\beta, \beta_1, \beta_{01}) \in \mathbb{R}^3$ such that

$$\begin{aligned}f_{001}(x) - u_{\max}\, f_{101}(x) &= \alpha f_0(x) + \alpha_1 f_1(x) + \alpha_{01} f_{01}(x),\\ f_{001}(x) + u_{\max}\, f_{101}(x) &= \beta f_0(x) + \beta_1 f_1(x) + \beta_{01} f_{01}(x).\end{aligned}$$

By linearity of the determinant, we have

$$\begin{aligned}D_{001}(x) - u_{\max}\, D_{101}(x) &= \alpha\, D_0(x),\\ D_{001}(x) + u_{\max}\, D_{101}(x) &= \beta\, D_0(x),\end{aligned}$$

and since $D_0(x) \neq 0$ then we can compute α and β along the trajectory. Besides, along any singular extremal, these quantitites can be linked to the signs of $\ddot{\Phi}_\pm(t)$:

$$\begin{aligned}\ddot{\Phi}_-(t) &= \langle p(t)\,, f_{001}(x(t)) - u_{\max}\, f_{101}(x(t))\rangle = \alpha(t)\, H_0(z(t)),\\ \ddot{\Phi}_+(t) &= \langle p(t)\,, f_{001}(x(t)) + u_{\max}\, f_{101}(x(t))\rangle = \beta(t)\, H_0(z(t)),\end{aligned}$$

with $H_0(z(t)) > 0$. Denoting t_0 the time when the extremal has a contact with the switching surface Σ_1, the behavior of the trajectory near z_0 is given by the signs of $\alpha(t_0)$ and $\beta(t_0)$. Indeed, the trajectory is

- Hyperbolic if $\alpha(t_0) < 0$ and $\beta(t_0) > 0$,
- Elliptic if $\alpha(t_0) > 0$ and $\beta(t_0) < 0$,
- Parabolic if $\alpha(t_0)\beta(t_0) > 0$.

3.3 Second-order optimality conditions

This section relies on the work of Bonnard and Kupka[7] about second-order optimality conditions.

Definition 4. Let $z(\cdot)$ be a reference singular solution of $\overrightarrow{h}_s$ on $[0\,, t_f]$ and contained in Σ_s. The variational equation

$$\begin{aligned} \delta\dot{z}(t) &= \mathrm{d}\overrightarrow{h}_s(z(t)) \cdot \delta z(t), \\ \mathrm{d}H_1(z(t)) \cdot \delta z(t) &= \mathrm{d}H_{01}(z(t)) \cdot \delta z(t) = 0, \end{aligned}$$

is called Jacobi equation. A Jacobi field $J(\cdot) \coloneqq (\delta x(\cdot), \delta p(\cdot))$ is a non-zero solution of the Jacobi equation. It is said semi-vertical at time t if $\delta x(t) \in \mathbb{R} f_1(x(t))$. The time $0 \leq t_1 \leq t_f$ is said to be conjugate if there exists a Jacobi field $J(\cdot)$ semi-vertical at $t = 0$, $t = t_1$ and the points $x_0 = x(0)$ and $x_1 = x(t_1)$ are said to be conjugate.

Assumption 3.5. *Let $z(\cdot) = (x(\cdot), p(\cdot))$ be a reference singular extremal curve on $[0\,, t_f]$ solution on Σ_s and we assume the following:*

- *$f_0(x)$ and $f_1(x)$ are linearly independant along $x(\cdot)$. $H_{101}(z(\cdot))$ is not equal to zero along $z(\cdot)$ and $x(\cdot)$ is injective.*
- *The space $K(t) \coloneqq \left\{ \mathrm{ad}^k f_0 \cdot f_1(x(t)) \;\middle|\; k = 0, \ldots, n-2 \right\}$ has codimension one, where $\mathrm{ad}^0 f_0 \cdot f_1(x(t)) = f_1(x(t))$ and $\mathrm{ad} f_0 \cdot f_1(x(t)) = f_{01}(x(t))$.*
- *$h_s(z(t)) = \langle p(t)\,, f_0(x(t)) + u_s(z(t)) f_1(x(t)) \rangle$ is not equal to zero along $z(\cdot)$.*

Then we have the following theorem in the case of a single-input affine system.

Theorem 3.6. *Let consider t_c the first conjugate time. Under assumptions 3.5, the reference singular trajectory $x(\cdot)$ is C^0-locally time minimizing in the hyperbolic case and time maximizing in the elliptic case on $[0\,, t_c)$.*

Remark 3. Moreover, the trajectory $x(\cdot)$ is not time optimal in L^∞-topology on $[0\,, t]$, for every $t > t_c$.

From now on, the sufficient conditions of optimality come down to the search of the first conjugate time t_c. In the case of an affine system in dimension 3, the singular control is independent of the adjoint variable p and we can give the following characterization of a Jacobi field $J(\cdot)$ along the state variable $x(\cdot)$, assuming that $x(\cdot)$ is a singular trajectory contained in the set $\left\{ x \in \mathbb{R}^3 \;\middle|\; D_{101}(x) \neq 0 \right\}$ on $[0\,, t_f]$.

Proposition 3.7. *A Jacobi field $J(\cdot)$ along $x(\cdot)$ for a three dimensional system is a non trivial solution of the variational equation*

$$\begin{aligned} \delta\dot{x}(t) &= \frac{\partial}{\partial x}(f_0 + u_s\, f_1)(x(t)) \cdot \delta x(t), \\ \delta x(0) &\in \mathbb{R} f_1(x(0)). \end{aligned}$$

Then the first conjugate time is the first time $t_c > 0$ such that

$$\det(J(t_c), f_0(x(t_c)), f_1(x(t_c))) = 0,$$

since by assumption f_0 and f_1 are linearly independent and J is colinear at f_1 only at the times 0 and t_c.

4. Application to a medium-haul aircraft

4.1 Solving $(\mathcal{P}_{t_f})$ with direct and indirect numerical methods

4.1.1 Numerical methods

For small-time trajectories, near the switching surface the parabolic, elliptic and hyperbolic classification is valid. On the other hand, "long"-time optimal trajectories, *i.e.* solution of $(\mathcal{P}_{t_f})$, must minimize the travel time on each sub-interval no matter what the length of the interval is. From this fact, we consider that the time-optimal climbing trajectory is composed of a concatenation of hyperbolic, parabolic or elliptic arcs. Two types of numerical methods are used in order to solve the problem $(\mathcal{P}_{t_f})$: a direct method to determine the optimal structure and to get a good initial guess (see figure 1) in order to make the indirect method converge (see figure 3) which gives a refined solution and make possible a fine analysis of the problem (see figure 8).

Firstly, we use the so-called direct approach wich consists in transforming the infinite dimensional optimal control problem $(\mathcal{P}_{t_f})$ into a finite dimensional optimization problem (NLP). This is done by a discretization in time

applied to the state and control variables, as well as the dynamics equation. These methods are usually less precise than indirect methods based on Pontryagin's Maximum Principle, but more robust with respect to the initialization. Also, they are more straightforward to apply, hence their wide use in industrial applications. We refer the reader to for instance the books of Betts[3] and Gerdts[11] for more details on direct transcription methods and NLP algorithms. About the direct methods, all the tests were run using the *Bocop*[4] software and the discretized nonlinear optimization problems were solved by the well-known *Ipopt*[21] solver.

When the structure of the solution is known, we use indirect methods to refine the solution. More precisely, we use multiple shooting techniques which consists in solving a Multi-Point Boundary Value Problem (MPBVP) obtained from the application of the maximum principle. The MPBVP is then transformed into a system of nonlinear equations which is solved by a Newton-like algorithm. See the book of Bulirsch and Stoer[8] for details about indirect methods. About the indirect methods, all the tests were run using the *HamPath*[9] software and the system of nonlinear equations were solved by the *hybrj*[17] routine.

4.1.2 Numerical results

In this paper, the direct methods are used to determine the structure of the trajectory and to initialize the indirect methods. The figure 1 shows the resulting control for a middle-haul aircraft. This solution is computed using a gauss scheme of order 4 with 750 nodes of discretization. The final time is $t_f \approx 654$ s and the data which describes the aircraft and the atmosphere are presented in table 1. This aircraft starts from $x_0 = (3480, 128.6, 69000)$ up to the beginning of the cruise defined by $x_f = (9144, 191, 68100)$.

Data	Value	Unit	Data	Values	Unit
S	1.226×10^2	m^2	Θ_0	2.882×10^2	K
$C_{D,0}$	2.42×10^{-2}		β	6.500×10^{-3}	$K.m^{-1}$
$C_{D,1}$	4.690×10^{-2}		P_0	1.013×10^6	Pa
$C_{T,1}$	1.410×10^5	N	g_0	9.810	$N.m^{-1}$
$C_{T,2}$	4.892×10^4	ft	R	2.880×10^2	$J.kg^{-1}.K^{-1}$
$C_{T,3}$	6.500×10^{-11}	ft^{-2}	γ_{air}	1.4	
$C_{S,1}$	6.333×10^{-1}	$kg.min^{-1}.kN^{-1}$	$\kappa := \gamma_{\text{air}}/(\gamma_{\text{air}} - 1)$	2.857×10^{-1}	
$C_{S,2}$	8.590×10^{-2}	kts			

Table 1: Constant data of a middle-haul aircraft and constant data of the atmospheric model during the climbing phase.

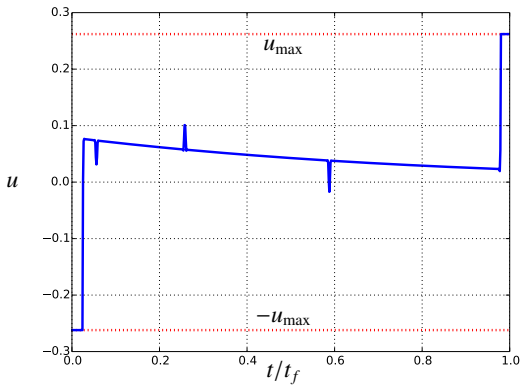

Figure 1: Control law for a time-optimal trajectory using direct methods obtained with a gauss discretization scheme of order 4 using 750 nodes. The control seems to follow a structure of the form $\sigma_-\sigma_s\sigma_+$.

The resulting control seems to be of the form $\sigma_-\sigma_s\sigma_+$, this structure reminds the hyperbolic case where the structure of the control is given by $\sigma_\pm\sigma_s\sigma_\pm$. Let check this structure with the indirect methods. The *HamPath* software computes from the maximized Hamiltonian the corresponding adjoint system thanks to automatic differentiation.

Hence, we need to introduce the following true Hamiltonians

$$h_{\pm}(x,p) \coloneqq H_0(x,p) \pm u_{\max} H_1(x,p),$$
$$h_s(x,p) \coloneqq H_0(x,p) + u_s(x) H_1(x,p),$$

with u_s given by eq. (10) and which composed the maximized Hamiltonian

$$\mathcal{H}(x(t),p(t)) \coloneqq \begin{cases} h_-(x(t),p(t)), \text{ when } 0 \leqslant t < t_1, \\ h_s(x(t),p(t)), \text{ when } t_1 \leqslant t < t_2, \\ h_+(x(t),p(t)), \text{ when } t_2 \leqslant t \leqslant t_f, \end{cases}$$

where t_1 and t_2 represent the switching times.

Remark 4. All the needed expressions of determinants and vector fields, for instance $D_{001}(x)$, $D_{101}(x)$ or $f_{01}(x)$, may be found in the work of Ref.[12]

Finally, we define the shooting function $S : \mathbb{R}^{5n+3} \to \mathbb{R}^{5n+3}$

$$S(p_0,t_1,t_2,t_f,z_1,z_2) \coloneqq \begin{pmatrix} x_f - \pi_x(z(t_f,z_2,t_2)) \\ \mathcal{H}(z(t_f,z_2,t_2)) + p^0 \\ H_1(z_1) \\ H_{01}(z_1) \\ z_2 - z(t_2,z_1,t_1) \\ z_1 - z(t_1,z_0,0) \end{pmatrix} \tag{11}$$

where $z_0 \coloneqq (x_0,p_0)$, $\pi_x(x,p) = x$, $z(t_j,z_i,t_i)$ is the solution[1] at t_j of the initial value problem $\dot{z}(t) = \overrightarrow{\mathcal{H}}(z(t))$, $z(t_i) = z_i$. The two first conditions represent the boundary conditions of the climbing problem. The third and the fourth conditions are related to the structure of the control and the two final conditions are matching conditions. The shooting method consists in finding a zero of $S(y)$ with $y \coloneqq (p_0,t_1,t_2,t_f,z_1,z_2)$. To any zero of S is associated a unique BC-extremal of $(\mathcal{P}_{t_f})$. The *HamPath* software is used to solve the shooting equation $S(y) = 0$ and we find y^* such that $\|S(y^*)\| \approx 1.07 \times 10^{-10}$. The solution y^* is composed of $p_0^* \approx (4.09 \times 10^{-2}, 6.00 \times 10^{-1}, -1.92 \times 10^{-1})$, $t_1^* \approx 19$ s, $t_2^* \approx 642$ s and $t_f^* \approx 656$ s. The values of z_1^* and z_2^* are omitted as they can be computed by numerical integration. Figures 2 and 3 depict the evolution of the altitude, the velocity and the air slope (which is the control in our dynamics) associated to the $\sigma_-\sigma_s\sigma_+$ structure.

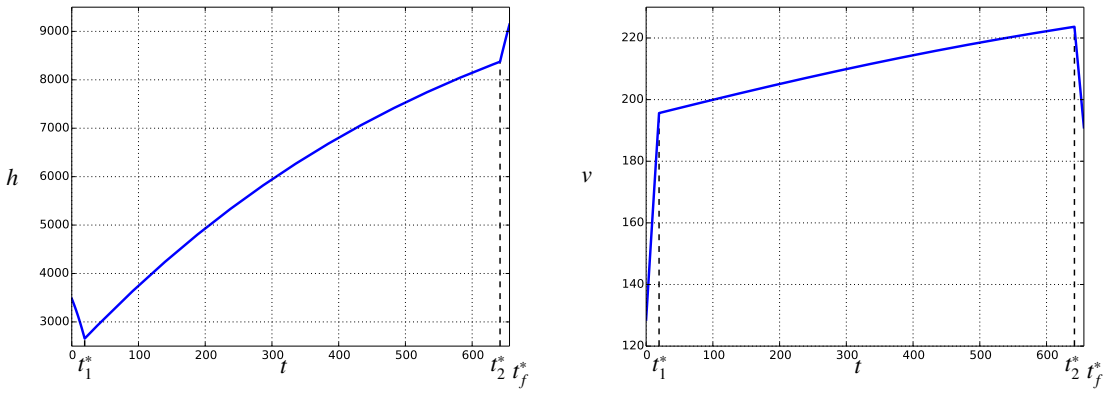

Figure 2: Evolution of the altitude h and of the true air speed v associated to the $\sigma_-\sigma_s\sigma_+$ structure. At the boundaries of the trajectory, we observe that h and v have opposite variation, for example when the altitude is decreasing the true air speed is increasing. This behavior looks like an energy sharing strategy where, at the beginning of the trajectory, potential energy is transformed into kinetics energy whereas the opposite exchange happens at the end of the trajectory.

[1] Numerically, $z(t_j,z_i,t_i)$ is computed with a high-order Runge-Kutta scheme with adaptative step-size.

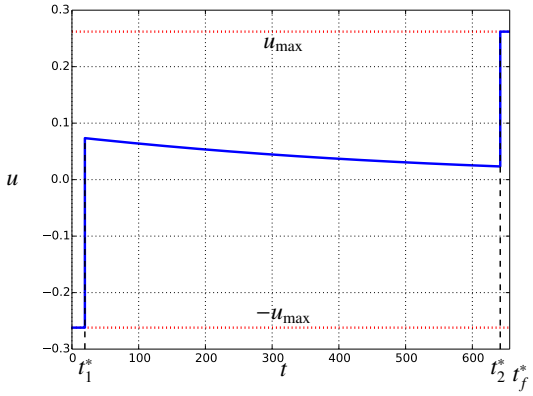

Figure 3: Evolution of the control law associated to the $\sigma_-\sigma_s\sigma_+$ structure.

In a second time, we check *a posteriori* that the trajectory is hyperbolic by computing the values of $\alpha(\cdot)$ and $\beta(\cdot)$, defined on section 3.2, along the singular arc. The validity of the generalized Lendendre-Clebsch condition, see corollary 3.4, along the trajectory is also checked. At the same time, we compute the quantity $\Lambda(\cdot) \coloneqq \det(J(\cdot), f_0(x(\cdot)), f_1(x(\cdot)))$ in order to check the absence or presence of a conjugate time on $[t_1^*, t_2^*]$. The results of these computations are presented in figures 4 and 5. The values of $\alpha(\cdot)$ and $\beta(\cdot)$ on $[t_1^*, t_2^*]$ are consistent with the hyperbolic case. In addition, the hyperbolic trajectory satisfy the sufficient conditions of optimality since $\Lambda(t) \neq 0$ on $(t_1^*, t_2^*]$. In conclusion, this hyperbolic trajectory is locally a C^0-optimal trajectory.

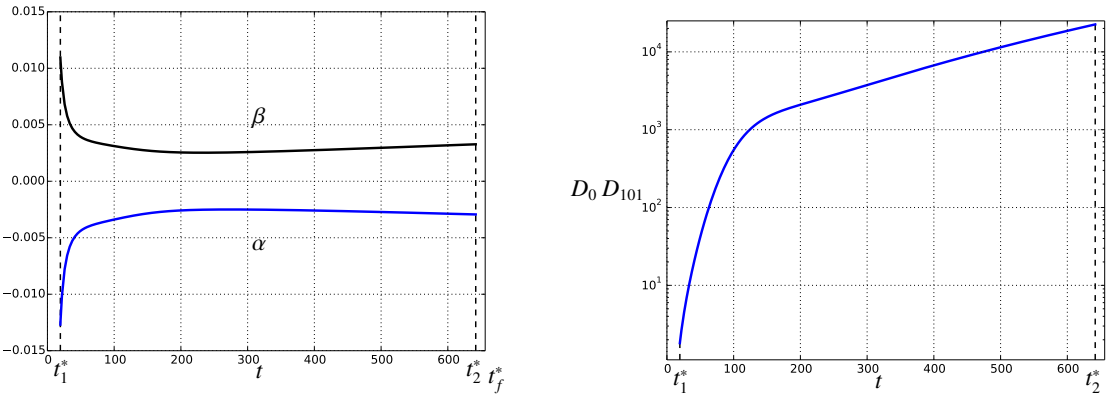

Figure 4: Evolution of the quantities $\alpha(\cdot), \beta(\cdot)$ and $D_0(x(\cdot))\, D_{101}(x(\cdot))$ along the singular arc. The generalized Legendre-Clebsch condition from corollary 3.4 is satisfied all along the singular arc as $D_0(x(\cdot)\, D_{101}(x(\cdot)) > 0$. The signs of $\alpha(\cdot)$ and $\beta(\cdot)$ along the singular arc confirm that we have an hyperbolic trajectory.

4.2 Small-time analysis at the beginning of the trajectory

From now on, we know that our hyperbolic trajectory is locally time-optimal. In this section and the following, we intend to study the deformation of this trajectory with respect to some parameters, focusing our analysis on the hyperbolic case. We aim to study the influence of the initial and final conditions by fixing the initial speed, the initial altitude and the final altitude but making the initial mass m_0 and the final velocity v_f varying in predefined ranges ($m_0 \in [48\,000, 72\,000]$ kg and $v_f \in [190, 250]$ m.s^{-1}) which are admissible values for the chosen aircraft. Let emphasize that the final mass m_f is free. The goal now is to give the optimal structure depending on the two parameters m_0 and v_f. More precisely, we want to determine for a given couple (m_0, v_f), the type of the bang arcs at the beginning and the end of the trajectory. We present the analysis made at the beginning of the trajectory. In a similar way, we can study the end of the trajectory.

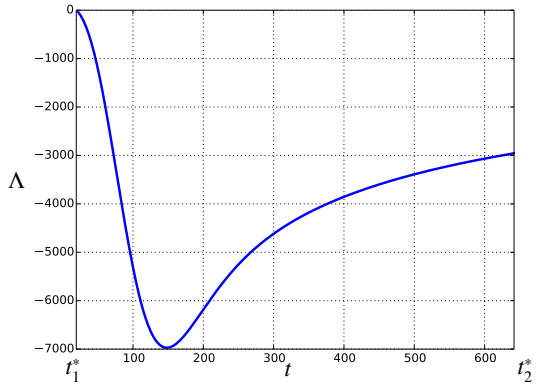

Figure 5: Evolution of $\Lambda(\cdot) = \det(f_0(x(\cdot)), f_1(x(\cdot)), J(\cdot))$ on $[t_1^*, t_2^*]$ where $J(\cdot)$ represents the Jacobi field. As $\Lambda(t) < 0$ for all t in $(t_1^*, t_2^*]$, we observe the absence of conjugate points on $[t_1^*, t_2^*]$ and then the singular arc in $\sigma_-\sigma_s\sigma_+$ is locally time-optimal.

In the aircraft dynamics, the mass m is considered as a slow variable. In other words, the mass m evolves much more slowly than the altitude and the velocity. Let consider small-time variation, the evolution of the mass can be omitted and then the dynamics can be reduced to a planar dynamics, given by

$$\dot{\bar{x}}(t) = \bar{f}_0(\bar{x}(t)) + u\bar{f}_1(\bar{x}(t)),$$

where $\bar{x} := (h, v)$ and

$$\bar{f}_0(\bar{x}) := \begin{pmatrix} 0 \\ \dfrac{T(h)}{m_0} - \dfrac{1}{2}\dfrac{\rho(h)Sv^2}{m_0}C_{D,0} - 2\dfrac{m_0 g_0^2}{\rho(h)Sv^2} \end{pmatrix}, \quad \bar{f}_1(\bar{x}) := \begin{pmatrix} v \\ -g_0 \end{pmatrix}.$$

Let consider the beginning of the trajectory and let $\bar{x}_0 := (h_0, v_0)$ denote the initial point of this dynamics associated to the initial constant mass m_0. The singular set in dimension 2, which contains the singular extremals, is given by $S := \{\bar{x} \in \mathbb{R}^2 \mid \det(\bar{f}_1(\bar{x}), \bar{f}_{01}(\bar{x})) = 0\}$. It depends on m_0 and locally if 0 is a regular value of the application $\bar{x} \mapsto \Psi(\bar{x}) := \det(\bar{f}_1(\bar{x}), \bar{f}_{01}(\bar{x}))$, then each connected component of $\Psi = 0$ is diffeomorphic to the circle or the real line. Let assume there exists only one connected component diffeomorphic to the real line and let consider a point $\bar{x}_0 \notin S$. Then, two cases may occur: either $\bar{x}_0$ is below the line which represents S or it is above.

The figure 6 depicts the behavior of the negative bang and positive bang trajectories from $\bar{x}_0$. Since the full trajectory is of the form $\sigma_\pm\sigma_s\sigma_\pm$, the purpose of the bang arcs is to connect the singular arc. Then if $\bar{x}_0$ is below S, according to figure 6, an arc σ_- must begin the trajectory. On the other hand if $\bar{x}_0$ is above S, an arc σ_+ must begin the trajectory. For a given mass m_0 and a given altitude h_0, we denote by v_0^S the associated velocity such that the point $(h_0, v_0^S) \in S$. The figure 7 shows the evolution of v_0^S for $m_0 \in [48\,000, 72\,000]$. In this figure we compare v_0^S and v_0. Since v_0 is constantly equal to 128.6 $\mathrm{m.s}^{-1}$ we observe that $v_0^S > v_0$ for every m_0 in $[48\,000, 72\,000]$. As a consequence, in any case the point $\bar{x}_0 = (h_0, v_0)$ is below the line which represents the singular set S and then we must start with a negative bang. The same argumentation may be used at the end of the trajectory to determine the nature of the final bang. In our situation, we can have both cases $\sigma_-\sigma_s\sigma_\pm$ depending on the value of v_f.

4.3 Local classification of the optimal structure with respect to $\bar{m}_0$ and v_f

Locally, we search BC-extremals of the form $\sigma_-\sigma_s\sigma_\pm$. Let consider the separating trajectory $\sigma_-\sigma_s$. We note again $\mathcal{H}$ the maximized Hamiltonian associated to this structure, and it is defined by

$$\mathcal{H}(z(t)) := \begin{cases} h_-(z(t)), \text{ when } 0 \leqslant t < t_1, \\ h_s(z(t)), \text{ when } t_1 \leqslant t \leqslant t_f. \end{cases}$$

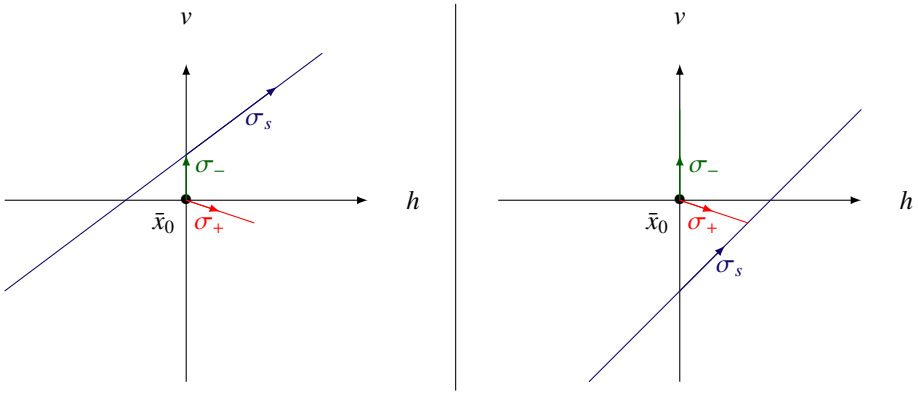

Figure 6: Local representation of the negative bang (the green curve) and the positive bang (the red curve) trajectories from $\bar{x}_0$. On the left (resp. right), $\bar{x}_0$ is located below (resp. above) the blue line which represents locally the singular set S. On the left figure, the only way to connect the singular trajectory σ_s, which is time-optimal, is to follow an arc σ_- whereas on the right figure the only way to connect σ_s is to follow an arc σ_+.

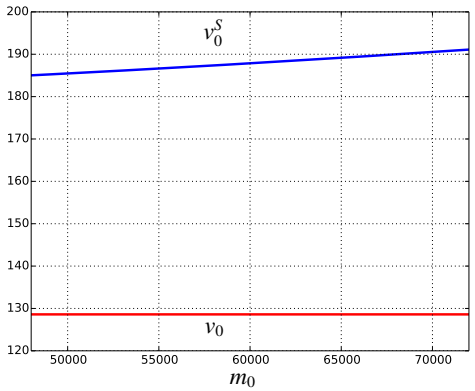

Figure 7: Representation of v_0 and v_0^S in relation with the initial mass variation. The quantity v_0^S is computed such that $\hat{x}_0 = (h_0, v_0^S) \in S$ with h_0 fixed and $m_0 \in [48\,000\,, 72\,000]$. The sign of the quantity $v_0^S - v_0$ indicates if the initial point $\bar{x}_0$ is above or below the singular set S. We observe that $v_0^S - v_0 > 0$ for all m_0 and then $\bar{x}_0$ is below the singular set S for every $m_0 \in [48\,000\,, 72\,000]$.

The shooting function denoted S_{-s} associated to this trajectory is defined by

$$S_{-s}(p_0, t_1, t_f, z_1) := \begin{pmatrix} h_f - h(t_f; t_1, z_1) \\ \mathcal{H}(z(t_f; t_1, z_1)) + p^0 \\ p_m(t_f; t_1, z_1) \\ H_1(z_1) \\ H_{01}(z_1) \\ z(t_1; 0, z_0) - z_1 \end{pmatrix}$$

where $z_0 := (x_0, p_0)$, $z(t_j; t_i, z_i)$ is the solution at t_j of the initial value problem $\dot{z}(t) = \vec{\mathcal{H}}(t)$, $z(t_i) = z_i$ and p_m is the adjoint variable associated to the mass m. The *HamPath* package is used to solve the shooting equation $S_{-s}(y) = 0$, $y := (p_0, t_1, t_f, z_1)$, and we find $y^* := (p_0^*, t_1^*, t_f^*, z_1^*)$ such that $\|S(y^*)\| \approx 6.1 \times 10^{-9}$. The solution is composed of $p_0^* \approx (6.08 \times 10^{-2}, 1.12, -2.72 \times 10^{-2})$, $t_1^* \approx 78.7$ s and $t_f^* \approx 889$ s. The value z_1^* is omitted since it can be computed by numerical integration. The *HamPath* package may also be used to realize a differential continuation on a parameter. See the book of Allgower and Georg[1] for details about differential path-following methods and we refer to the presentation of the software[9] for details about the implementation of these methods in the *HamPath* code. We use this functionality on the initial mass from $m_0 = 72\,000$ kg up to $m_0 = 48\,000$ kg. The figure 8 depicts locally the structure of the trajectories in relation with the initial mass and the final velocity. The blue curve, computed by numerical continuation, represents all the trajectories which end on the singular set. As the final altitude h_f is fixed, the final velocity v_f of each

of these trajectories is adjusted to be on this set. We note v_{f,m_0} the final velocity associated to the initial mass m_0 for which the associated trajectory ends on the singular set. This particular trajectory is the boundary between $\sigma_-\sigma_s\sigma_-$ and $\sigma_-\sigma_s\sigma_+$ trajectories. The classification given in figure 8 shows that if v_f is below v_{f,m_0}, the final bang is a positive one and if v_f is above v_{f,m_0} it is a negative one.

Remark 5. It has not been proven that this classification gives time-optimal trajectories but we may emphasize that the reference trajectory, from section 4.1.2, satisfies necessary and sufficient conditions of local optimality and we mention that this classification has been obtained thanks to an analysis of small-time optimal trajectories.

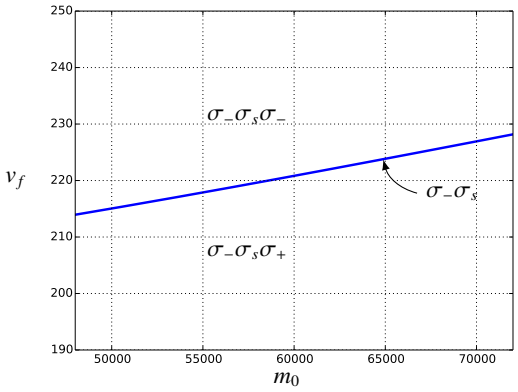

Figure 8: Local classification of the optimal structure with respect to the initial mass and the final velocity of the climbing phase. Note that this final velocity is also the cruise velocity.

5. Conclusion

In this paper, the time-optimal control problem of an aircraft in its climbing phase is modeled as a Mayer problem. Firstly, the four dimensional dynamics is reduced into a three dimensional dynamics to deal with the singular perturbation phenomenon. This reduced system is a single-input control system where the control appears linearly. The behavior of bang-bang extremals near the switching surface with the characterization of the singular trajectories are studied in the particular case of the dimension 3 throughout geometric analysis. Combining these results with numerical methods and small-time considerations leads to sketch a local classification of fairly time-optimal climbing trajectories depending on the initial mass and the cruise speed.

This study does not take into account states constraints which should be fulfilled during the climbing phase. For instance, the *Computed Air Speed* (CAS) and the number of mach (M) are limited by the *Operation Maximal Speed* (VMO) and by the *Maximal Mach Operation* (MMO). The figure 9 shows the evolution of the two velocity constraints $c_1(x) \coloneqq \mathrm{CAS}(x) - \mathrm{VMO}$ and $c_2(x) \coloneqq \mathrm{M}(x) - \mathrm{MMO}$ for a trajectory of the form $\sigma_-\sigma_s\sigma_+$ with $m_0 = 69\,000$ kg and $v_f = 191$ m.s^{-1}. In this example none of these constraints are saturated but a more exhaustic study is necessary to understand the behavior of the trajectories in presence of state constraints. A methodology closed to the unconstrained case can be applied except that the geometric study should be based on a maximum principle with state constraints which is presented, for example, in the work of Jacobson[13] *et al.* and Maurer.[16] Besides, the small-time considerations could also be used and could give some interesting results on the structure of time-optimal trajectory with state constraints as it was done for the space shuttle reentry problem in the work of Bonnard *et al.*[6]

References

[1] E. Allgower and K. Georg. *Introduction to numerical continuation methods*, volume 45 of *Classics in Applied Mathematics*. Soc. for Industrial and Applied Math., Philadelphia, PA, USA, 2003.

[2] M. D. Ardema. *Singular perturbations in flight mechanics*. Thèse de doctorat, 1977.

[3] J. T. Betts. *Practical Methods for Optimal control Using Nonlinear Programming*. Advances in Design and Control. Soc. for Industrial and Applied Math., Berlin, Heidelberg, New-York, 2001.

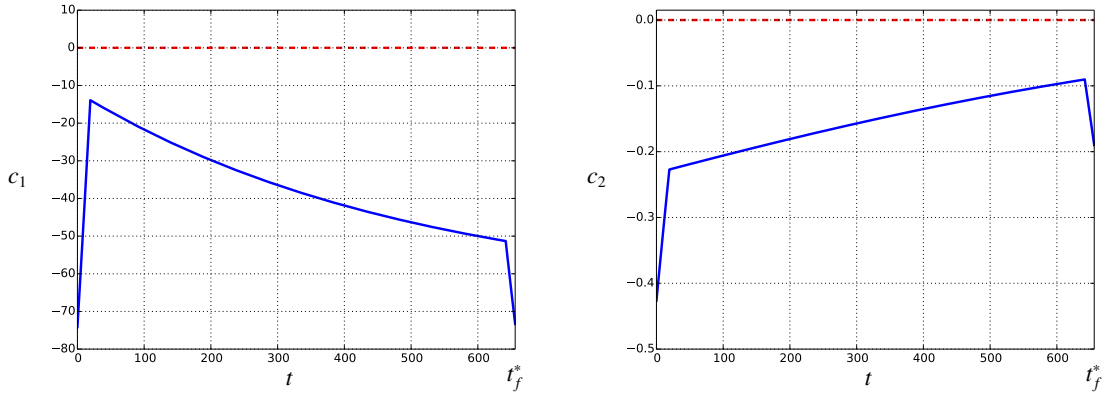

Figure 9: Evolution of the speed constraints c_1 and c_2 along the time-optimal trajectory associated to the structure $\sigma_-\sigma_s\sigma_+$. All along the trajectory none of these constraints are saturated.

[4] J. F. Bonnans, D. Giorgi, V. Grelard, B. Heymann, S. Maindrault, P. Martinon, and O. Tissot. Bocop - a collection of examples. Technical report, INRIA, 2016.

[5] B. Bonnard and M. Chyba. *Singular Trajectories and their Role in Control Theory*. Springer-Verlag, Berlin, Heidelberg, Paris, 2003.

[6] B. Bonnard, L. Faubourg, G. Launay, and E. Trélat. Optimal control with state constraints and the space shuttle re-entry problem. *J. Dyn. Control Syst.*, 9(2):155–199, 2003.

[7] B. Bonnard and I. Kupka. Théorie des singularités de l'application entrée/sortie et optimalité des trajectoires singuliéres dans le problème du temps minimal. *Forum Math.*, 5(2):111—159, 1993.

[8] R. Bulirsch and J. Stoer. *Introduction to numerical analysis*. Springer, New-York, 2002.

[9] J.-B. Caillau, O. Cots, and J. Gergaud. Differential continuation for regular optimal control problems. *Optim. Methods Softw.*, 27(2):177–196, 2012.

[10] O. Cots, J. Gergaud, and D. Goubinat. Time-optimal aircraft trajectories in climbing phase and singular perturbations (regular paper). In *IFAC World Congress, Toulouse, 09/07/2017-14/07/2017*, 2017.

[11] M. Gerdts. *Optimal control of ODEs and DAEs*. De Gruyter Textbook, 2011.

[12] D. Goubinat. *Contrôle optimal géométrique et méthodes numériques: application à un problème de montée d'un avion*. Thèse de doctorat, INP-ENSEEIHT, juin 2017.

[13] D. H. Jacobson, M. M. Lele, and J. L. Speyer. New necessary conditions of optimality for control problems with state-variable inequality constraints. *J. Math. Anal. Appl.*, 35:255–284, 1971.

[14] A. J. Krener. The high order maximal principle and its application to singular extremals. *SIAM J.Control Optim.*, 1(299):256–293, 1977.

[15] I. Kupka. Geometric theory of extremals in optimal control problems. i. the fold and maxwell case. *Trans. Amer. Math. Soc.*, 299(1):225–243, 1987.

[16] H. Maurer. On optimal control problems with bounded state variables and control appearing linearly. *SIAM J. Cont. Optim.*, 15(3):345–362, 1977.

[17] J. J. Moré, B. S. Garbow, and K. E. Hillstrom. User guide for minpack-1. Technical Report ANL-80-74, Argonne National Library, 1980.

[18] N. Nguyen. Singular arc time-optimal climb trajectory of aircraft in a two-dimensional wind field. *AIAA Guidance, Navigation and Control Conference and Exhibit*, 2006.

[19] D. Poles. Base of Aircraft DAta (BADA) aircraft performance modelling report. Technical Report 2009-09, Eurocontrol, september 2009.

[20] L. Pontriaguine, V. Boltianski, R.Gamkrélidizé, and E. Mitchenko. *Théorie mathématiques des processus optimaux*. Editions Mir, Moscou, 1974.

[21] A. Wachter and L. T. Biegler. On the implementation of a primal-dual interior point filter line search algorithm for large-scale nonlinear programming. *Math. Program.*, 106(1):25–57, 2006.